SIC POWER DEVICES IN POWER ELECTRONICS: AN OVERVIEW

Luciano F. S. Alves[1], Ruan C. M. Gomes[1], Pierre Lefranc[2], Raoni de A. Pegado[3], Pierre-Olivier Jeannin[2], B. A. Luciano[1], and Filipe V. Rocha[3]
[1]Federal University of Campina Grande (UFCG), Campina Grande - PB, Brazil
Emails: [luciano.alves, ruam.gomes]@ee.ufcg.edu.br, benedito@dee.ufcg.edu.br
[2]University Grenoble Alpes, G2Elab, F-38000 Grenoble, France
Emails: [Pierre.Lefranc, pierre-olivier.jeannin] @g2elab.grenoble-inp.fr
[3]Federal University of Paraíba (UFPB), João Pessoa-PB, Brazil
Emails: [raoni.pegado, filipe.rocha]@cear.ufpb.br

***Abstract* - Silicon (Si) power devices have dominated the world of Power Electronics in the last years, and they have proven to be efficient in a wide range of applications. But high power, high frequency and high temperature applications require more than Si can deliver. With the advance of technology, Silicon Carbide (SiC) and Gallium Nitride (GaN) power devices have evolved from immature prototypes in laboratories to a viable alternative to Si-based power devices in high-efficiency and high-power density applications. SiC and GaN devices have several compelling advantages: high-breakdown voltage, high-operating electric field, high-operating temperature, high-switching frequency and low losses. This paper provides a general review on the properties of these materials comparing some performance between Si and SiC devices for typical power electronics applications. Based on studied information, line of progress and the current state of developing, SiC seems to be the most viable substitute in high power and high temperature applications in the mid-term of Si, due to the fact that the GaN is still used in a reduced number of applications.**

I. INTRODUCTION

In power electronics, improving the efficiency of electronic devices is crucial to reduce switching losses. Nowadays, Silicon (Si) is by far the most widely used semiconductor material for power devices. However, the intrinsic physical properties of silicon have limitations that in some domains will prevent devices based on Si material from being the candidates for the future of power electronics. As Si-based power devices are approaching their material limits, engineers and researchers have prompted a lot of e□orts to find alternatives to Si-based power devices for better performance [1].

The search for a solution to the limitations of silicon leads to investigations of wide bandgap (WBG) semiconductors, such as Silicon Carbide (SiC) and Gallium Nitride (GaN) power devices. In comparison to Si, the main benefits of these materials are good operation over a wide temperature range, high dielectric strength and high saturation drift velocity. SiC power components have been the subject of extensive research in the last fifteen years. SiC has become the material of choice for next generation power semiconductor devices to replace existing Si technology. The wider bandgap, higher thermal conductivity, and larger critical electric feild allow SiC devices to operate at higher temperature, higher current density, and higher blocking voltage [2]-[15].

Silicon carbide is comprised of equal parts silicon and carbon via covalent bonding. Since this process will lead to a highly ordered confguration, a single crystal SiC is extremely hard; in fact it is known to be the third hardest substance on earth. There are more than 170 di□erent polytypes. Depending on the polytype crystal structure, the energy gap of silicon carbide varies from 2 to 3.3 eV. Among them, 4H and 6H are of interest technologically since large wafers can be made in this material, and hence used for device production [16]-[17]. Thus, in Section II an overview of the theoretical limits for power devices is given. Section III shows a short overview of the physical properties of Si, 4H-SiC, and GaN materials. The most promising commercial SiC power devices are analyzed in Section IV.

II. THEORETICAL LIMITS FOR POWER DEVICES

The theoretical limits for power devices translates the behavior of the semiconductors according to their breakdown voltage. In power electronics, the theoretical limits define the relationship between this voltage and the conduction resistance of the semiconductor, which translates into loss as a function of the application voltage on the device.

When the voltage in a power device increases, the electric field inside this device also increases. Since the electric field approaches a critical level *Ec*, the power device tends to suffer an avalanche effect. To allow simple comparison between similar systems with different material compositions, an abrupt one-dimensional P+/N diode , as shown in Fig. 1, is studied [18]. In this case, it's assumed that the voltage is only supported through one side of the structure. This assumption is valid for a P + N junction since the doping concentration on one side is very high in comparison with the other. Furthermore, since the P+ region is very thin and highly doped compared to the N region, the depletion region extends mainly in the doped region N, When this diode is reverse polarized, a depletion region is formed in the N region (depletion in the P+ region may be neglected). The electric field in the depletion region can be extracted from the Poisson equation [18]:

978-1-5090-6248-5/17/$31.00 ©2017 IEEE

$$\nabla^2 V = -\frac{\rho}{\varepsilon_s} \tag{1}$$

$$E = -\nabla V \tag{2}$$

Where V is the electrostatic potential, ρ is the charge density, ε_s is the dielectric constant of the semiconductor and E is the electric field.

Considering only the one-dimensional case, it has:

$$\frac{d^2V}{dx^2} = -\frac{dE}{dx} = -\frac{\rho}{\varepsilon_s} = -\frac{qN_D}{\varepsilon_s} \tag{3}$$

The charges within the depletion region, due to the presence of ionized donors, can be expressed as qN_D, where q is the charge of the proton and N_D represents the concentration of donors uniformly in the doped region N.

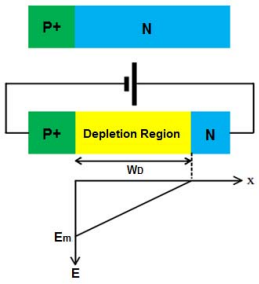

Fig. 1. Cross Section of an Abrupt Junction PN.

The solution of equation (3), using the boundary conditions $E(w_D) = 0$ and boundary $V(0) = 0$, produces the following expressions for the electric field and the electrostatic potential:

$$E(x) = -\frac{qN_D}{\varepsilon_s}(w_D - x) \tag{4}$$

$$V(x) = \frac{qN_D}{\varepsilon_s}\left(w_D x - \frac{x^2}{2}\right) \tag{5}$$

w_D can be related to the applied voltage using the condition, $V(w_D) = Va$, where Va is applied reverse voltage.

$$w_D = \sqrt{\frac{2\varepsilon_s V_a}{qN_D}} \tag{6}$$

In the break $V_a = V_R$ and, $Em = E(0) = E_c$ and then

$$w_D = \sqrt{\frac{2\varepsilon_s V_R}{qN_D}} \tag{7}$$

$$E_c = -\frac{qN_D}{\varepsilon_s} w_D \rightarrow w_D = -\frac{\varepsilon_s}{qN_D} E_c \tag{8}$$

Combining equations (7) and (8), it has :

$$N_D = \frac{\varepsilon_s {E_c}^2}{2qV_R} \tag{9}$$

$$w_D = -\frac{2V_R}{E_c} \tag{10}$$

The specific conduction resistance per unit area of the uniformly doped region is given by :

$$R_{on} = \frac{w_D}{q\mu_n N_D} \tag{11}$$

Combining equations (9) and (11), it has :

$$R_{on} = \frac{4V_R}{\varepsilon_s \mu_n {E_c}^3} \tag{12}$$

The denominator of equation (12), *i.e.*, $\varepsilon_s \mu_n {E_c}^3$ is an indicator of the impact of the properties of the semiconductor material on the conduction resistance. An exact modeling of specific conduction resistance requires consideration of dielectric strength and mobility dependence on doping concentration. In practice specific conduction resistance is calculated using the following approximations [16],[18]:

$$E_c \alpha N_D^{\gamma} \tag{13}$$

$$\mu_n \alpha N_D^{-x} \tag{14}$$

$$R_{on}\left(\Omega.\mathrm{cm}^2\right) \alpha V_R{}^n \tag{15}$$

$$n = \frac{2 - x - y}{1 - 2y} \tag{16}$$

For the Si: $R_{on}\left(\Omega.\mathrm{cm}^2\right) = 5.93 \times 10^{-9} {V_R}^5$ (17)

For the 4H-SiC: $R_{on}\left(\Omega.\mathrm{cm}^2\right) = 97 \times 10^{-12} {V_R}^5$ (18)

For the 6H-SiC: $R_{on}\left(\Omega.\mathrm{cm}^2\right) = 1.45 \times 10^{-11} {V_R}^6$ (19)

For the GaN: $R_{on}\left(\Omega.\mathrm{cm}^2\right) = 4 \times 10^{-12} {V_R}^5$ (20)

In Fig. 2 is shown the graph of equations (17)-(20). It is clear that the theoretical limit of high band-gap power devices is much higher than Si-based power devices. This means for the

same breakdown voltage these devices offer significantly less resistance in conduction. This characteristic makes the power converters made from SiC-based power devices more efficient, provided by reduction of switching losses as well as by conduction losses.

III. Physical Properties of Si, SiC and GaN

In power electronics, electrical quantities such as voltage, frequency and operating temperature define the application of the power system. In Table I is shown the physical properties of Si, 4H-SiC and GaN materials that determine these applications [19]–[21].

Some semiconductors are classified as "wide-bandgap" semiconductors because of their wider bandgap. Silicon has a bandgap of 1.1 eV and is not considered a wide bandgap semiconductor. The bandgaps of WBG semiconductors are about three times or more that of Si as can be seen in Table I . SiC polytypes and GaN have similar bandgap and electric field values, which are significantly higher than those of Si. WBG semiconductors have the advantage of high-temperature operation and more radiation hardening. As the temperature increases, the thermal energy of the electrons in the valence band increases. At a certain temperature, they have sufficient energy to move to the conduction band. This is an uncontrolled conduction that must be avoided. The temperature at which this happens is around 150°C for Si [18]. For WBG semiconductors, the bandgap energy is higher; therefore, electrons in the valence band need more thermal energy to move to the conduction band. This intrinsic temperature for SiC is around 900°C, The above reasoning is also true for radiation hardening. Radiation energy can also excite an electron like the thermal energy and make it move to the conduction band. As a result of the wide bandgap, devices built with WBG semiconductors can withstand more heat and radiation without losing their electrical characteristics. They can be used in extreme conditions where Si-based devices cannot be used [22].

WBG means a larger electric breakdown field (Ec). It results in power devices with higher breakdown voltages. With a high electric breakdown field, much higher doping levels can be achieved; thus, device layers can be made thinner at the same breakdown voltage levels [22]. The resulting WBG-semiconductor-based power devices are thinner than their Si-based counterparts and have smaller drift region resistances as can be seen in Fig. 2.

The high-frequency switching capability of a semiconductor material is directly proportional to its drift velocity. The drift velocities of WBG materials are more than twice the drift velocity of Si (1×10^7); therefore, it is expected that WBG semiconductor-based power devices could be switched at higher frequencies than their Si counterparts. Moreover, higher drift velocity allows charge in the depletion region of a diode to be removed faster; therefore, the reverse recovery current of WBG semiconductorbased diodes is smaller, and the reverse recovery time is shorter [22].

As explained earlier, because of the wide bandgap, WBG semiconductor-based devices can operate at high temperatures. In addition to this, SiC has another thermal advantage not mentioned previously — its high thermal conductivity. As seen in Eq. (21) [22], junction-to-case thermal resistance, R_{th-jc}, is inversely proportional to the thermal conductivity.

$$R_{th-jc} = \frac{d}{\lambda A} \tag{21}$$

where λ is the thermal conductivity, d is the length, and A is the cross-sectional area. Higher thermal conductivity means lower R_{th-jc}, which means that heat generated in a SiC-based device can more easily be transmitted to the case, heatsink, and then to the ambient; thus, the material conducts heat to its surroundings easily, and the device temperature increases more slowly. For higher-temperature operation, this is a critical property of the material. As seen in Table I, GaN has the worst thermal conductivity — even lower than that of Si.

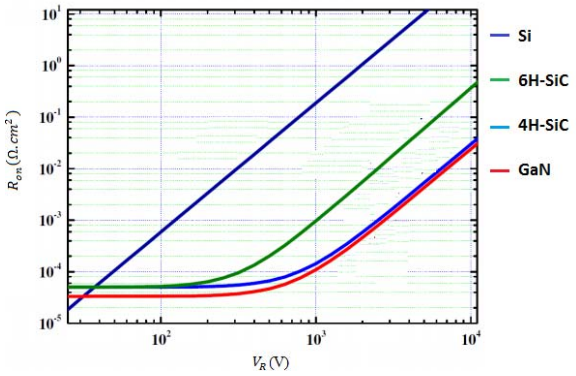

Fig. 2. On-State Resistance Versus Breakdown Voltage for Different Materials [16].

Table I

Physical Properties of Silicon (Si), Silicon Carbide (4H-SiC) and Gallium Nitride (GaN).

Electrical Property	Uni.	Si	4H-SiC	GaN
Band Gap Energy	eV	1.1	3.26	3.4
Electron Mobility	$cm^2/V.s$	1300	900	900-2000
Breakdown Field	V/cm	0.3×10^6	3×10^6	3.5×10^6
Saturation Drift Velocity	cm/s	1×10^7	2×10^7	2.5×10^7
Thermal Conductivity	W/cm.K	1.5	3.7	1.3

The analysis of the physical properties of the Si and the WBG semiconductors is shown in Fig. 3. High breakdown field and high band gap energy allow operation with high voltage and high temperature values. The high switching frequency is attributed to the high Saturation Drift Velocity and high electron mobility [23] –[27].

From Fig. 3 it can be concluded that the GaN power device is a good choice for high voltage and high switching frequency applications. However, it is not efficient at high temperature. On the other hand, the SiC is the best choice for high voltage, high switching frequency and high temperature applications.

IV. SiC Power Devices Review

In this section are reviewed the most promising commercial SiC power devices, including diode and Metal Oxide Semiconductor Field Effect Transistor (MOSFET). Some other types of devices such as the SiC Bipolar Junction Transistor (BJT), also provide excellent performance; however, they are less attractive from industry application perspective. Therefore, they are not covered in this section. The state-of-art research developments in the high voltage portfolio are reviewed, such as high voltage Insulated Gate Bipolar Transistor (IGBT) and gate turn-off (GTO) thyristor.

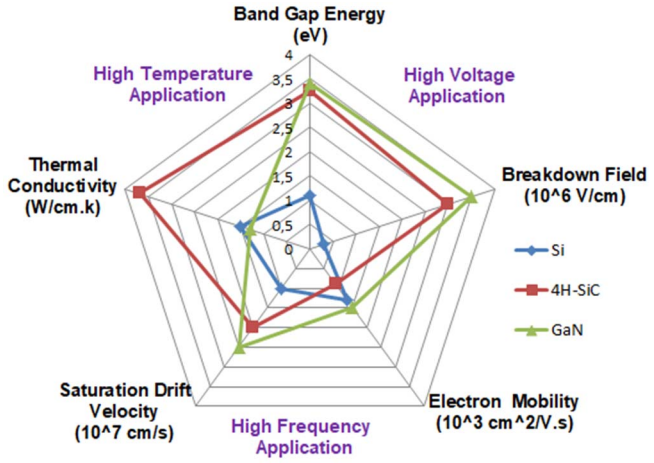

Fig. 3. Material properties comparison between Si, 4H-SiC and GaN.

A. SiC Diodes

There are three main types of SiC diodes: the SiC Schottky diode, the SiC junction barrier Schottky (JBS) diode, and the SiC PiN diode [28]. The basic structures are shown in Fig. 4.

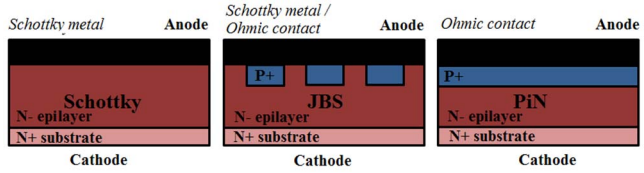

Fig. 4. Three basic SiC diode strctures [28].

The combination of a Schottky diode structure and SiC material makes the SiC Schottky barrier diode (SBD) an ideal replacement for the Si PIN diode. Due to the wide band-gap energy, the forward voltage drop of the SiC Schottky diode is 1~2 V, which is larger than its Si counterpart. Thus, the main advantage of SiC Schottky diode is obtained in high-voltage applications where the larger voltage drop has negligible impact on the losses. Another important characteristic of the SiC Schottky diode that is the opposite of its Si counterpart is that the forward voltage drop has positive thermal coefcient, *i.e.*, increases as temperature increases, it allows parallel connection of the Schottky diode to handle higher current [29].

In the SBD, the leakage current at higher temperatures increases quickly as result of the Schottky barrier lowering effect, as a result the blocking voltage of SiC SBDs is limited to a few hundred of volts. In the SiC JBS diode the off-state leakage current is reduced even at therated junction temperature, which is typically below 175 °C [30]. Because the device conduction is still via majority carrier electrons, the speed of the JBS is not compromised. Therefore, the JBS diode provides excellent performance over a wide range of voltages and high-frequency applications [31].

The bipolar SiC PiN diode is a very promising device for ultra–high-voltage ranges. The differential resistance of the SiC PIN diode is much smaller than that of the JBS diode and its much lower leakage current compared with the JBS or SBD, making it an ideal candidate for higher temperature operation. However, the SiC PIN is ineffective from the conduction point of view when the blocking voltages are below 3 kV because its ~3 V PN junction knee voltage [32]. SiC JBS diodes are preferred in these voltage ranges.

The switching characteristics of a Schottky diode constructed with SiC and a fast silicon diode, each 600 V/10 A, are shown in Fig. 5. The device switches rapidly from ON to OFF, and there is virtually no reverse recovery current as result of the majority carrier conduction mechanism. This extremely fast reverse recovery characteristic is its most significant advantage over the Si PIN diode. In addition to enabling potential efficiency improvements, the low reverse recovery current also significantly reduces the converter oscillation and the related electromagnetic interference (EMI) problem during diode turn-off [33].

B. SiC Power Switches

The SiC JFET was the first SiC power switch to be marketed since it is relatively easy to implement and there is no reliability problem of the gate oxide as observed in SiC MOSFETs. The JFET is normally an ON-type switch (also called depletion mode JFET) and fully turned o when the gate voltage is below the pinch-o voltage, *i.e.*, about -15 V. When turned on, it present an ON-resistance which can be minimized when the gate voltage is higher than zero as shown in Fig. 6. The normally-ON characteristic makes the JFET na undesirable power device in power applications. To turn the JFET into a safe OFF-state, it needs a complex design control circuit to

provide a negative VGS voltage. One common technique to address this problem is to use a cascode driver, where a low-voltage, high-current Si-MOSFET is connected to the source of SiC JFET [34]-[36]. Typically 30 V MOSFETs with several mΩ ON-resistance are used for the cascode confguration. During normal operation, the low-voltage MOSFET is conducting without signifcant contribution to the total ON state resistance.

The SiC MOSFET have traditionally suffered from poor oxidesemiconductor interface quality, which has led to large threshold voltage instability. The gate oxide also degrades at a temperature even below maximum junction temperature of a SiC device [35]. However, the SiC MOSFET is still an attractive device especially for high power applications due to its lower conduction resistance compared to Si MOSFET, its higher switching speed and their ability to operate at elevated temperatures [37]. In Fig. 7 is shown the comparison between Si and SiC MOSFET in terms of the area specific resistance as a function of the breakdown voltage . The body diode of the SiC MOSFET is a PN diode that has ~3 V forward voltage drop, about 5 times that of a Si PN junction diode. However,

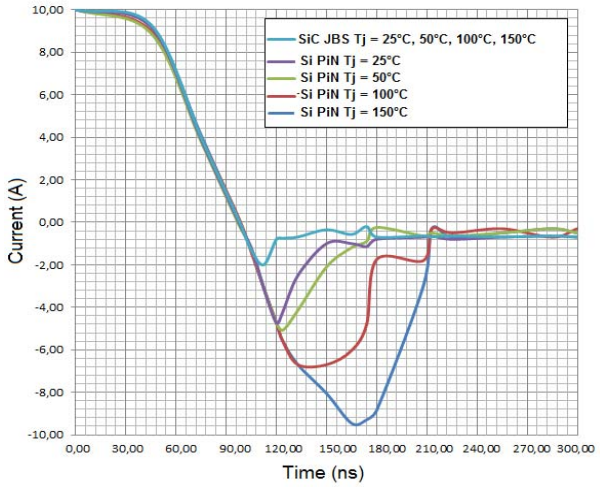

Fig. 5. Switching characteristics of a Schottky diode constructed with SiC and a fast silicon diode, each 600 V/10 A [33].

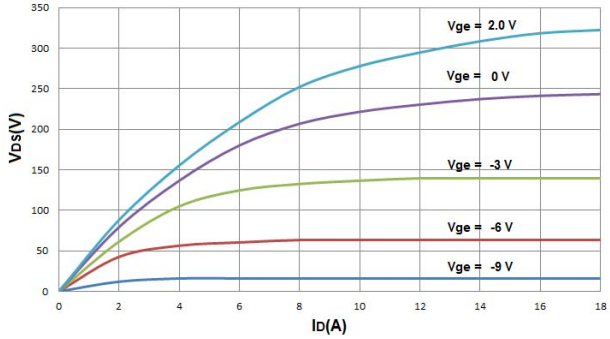

Fig. 6. Typical ID vs. VDS for di□erent gate voltage of Normally ON type 35 mΩ Rated 1200 JFET at 25°C [36].

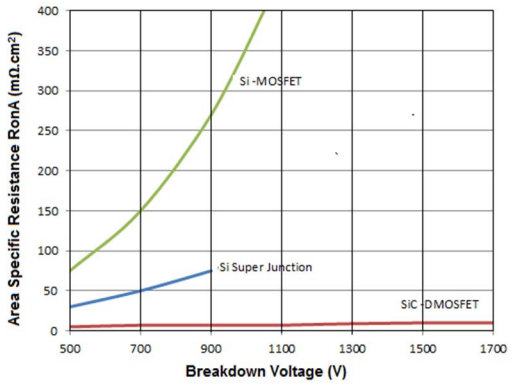

Fig. 7. Comparison between Si and SiC MOSFET [37].

reverse recovery time is much smaller compared to a Si PN diode. An advantage that resulted from the wide bandgap is that the ON-resistance of the SiC MOSFET increases by about 20 percent when the junction temperature increases from 25°C to 135°C, whereas that of the Si MOSFET increases by 250 percent [39].

The IGBT is the most widely used silicon device for power applications, with a very simple gate driver, low switching losses and high operating frequency. SiC MOSFET has been expected to replace Si IGBT since the high-voltage SiC MOSFET shows much reduced switching losses compared with the Si IGBT. However the voltage drop becomes unacceptable, especially for voltage levels higher than 10 kV [40]. In this condition, the combination of the SiC and bipolar device structure, such as SiC IGBT, would be desirable. Figure 8 shows typical cross section diagrams of N-type and P-type high-voltage SiC IGBTs. A buffer layer, or field stop layer, is needed to prevent field punch-through and to achieve high injection efficiency from the substrate. The P-IGBT have not

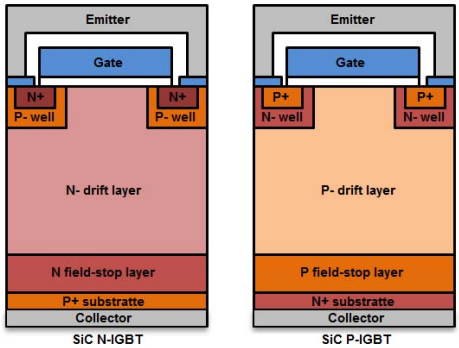

Fig. 8. Cross section structure of SiC IGBT [28].

demonstrated good performance, due to the difficulties in their manufacturing process. In addition, one of the features to be emphasized in SiC N-IGBTs is that they can be arranged in parallel, as they have a positive coefficient of conduction resistance temperature. However, theoretically, both N-IGBT and P-IGBT have similar direct voltage drops. Several high-voltage SiC IGBT designs have been reported [41]-[51]. The highest blocking voltage reported so far for a N-IGBT is 27 kV,

obtained by using a 230 µm drift layer [47]. The design also incorporated a lifetime enhancement process to reduce the voltage drop. The highest blocking voltage reported for a P-IGBT is 15 kV, as shown in [45]. The differential specific on-resistance for most of the reported SiC IGBTs is in the range of tens of mΩ.

The SiC GTO transistor is a promising SiC power device. It achieves the best current handling capability with a very low forward drop among all reported high-voltage SiC power devices, thanks to the double-side carrier injection and strong conductivity modulation [52]. In general, the advantages of higher impact of SiC GTO are: its ability to conduct high currents (tens of kA/cm^2) due to its superior thermal conductivity, its very low leakage current at high temperatures, wide bandgap, and its blocking capacity at high stresses [52]. With regard to its silicon correspondent, the SiC GTO provides the following benefits: reduction in the number of components and the complexity, weight and volume of the system, increased switching frequency, and efficient behavior at high temperature. Also, SiC GTO offers lower conduction resistance with respect to SiC MOSFET, SiC IGBT and Si IGBT. Based on SiC P-GTO technology, a 15 kV SiC ETO transistor has also been demonstrated [53]. The initial problem for the acceptance of SiC GTO was to the degradation of its voltage drop proportional to the time [54]. Nevertheless, efforts made to address this problem were effective and were able to maintain the direct voltage drop in an acceptable operating range even after 1000 hours, as shown in Fig. 9.

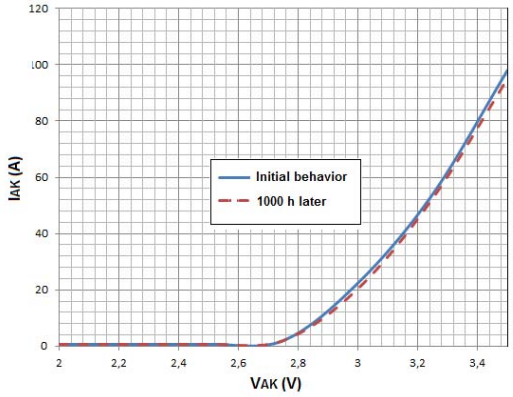

Fig. 9. Behavior of the V-I curve over time [52].

V. Conclusions

In this paper was presented the material characteristics of SiC wich allows several compelling advantages such as high breakdown voltage, high operating electric field, high operating temperature, high switching frequency, and low losses. The benefits and limitations of each commercially available SiC power devices were discussed together with comparisons with their Si counterparts. The performance of SiC devices have improved significantly and SiC power conversion systems are being accepted by industry. SiC Power devices technology is to a greater extent than GaN technology and is most important in research and commercialization efforts. The small improvement GaN provides great power not be sufficient to change gears and use GaN instead of SiC. SiC is the best transition material for future power devices where high temperature and high power is much needed.

Acknoledgements

The authors would like to thank the PPgEE/UFCG, the PPgEE/UFPB, the Grenoble Electrical Engineering laboratory (G2Elab), the National Council for Scientific and Technological Development (CNPq) and the Coordination of Improvement of Higher Education Personnel (CAPES).

References

[1] J. W. Palmour, “Silicon carbide power device development for industrial markets,” in Proc. IEEE IEDM., 2014, pp.1.1.1–1.1.8.

[2] J. Biela, M. Schweizer, S. Waffler, J. W. Kolar, “SiC versus Si—Evaluation of Potentials for Performance Improvement of Inverter and DC–DC Converter Systems by SiC Power Semiconductors,” Industrial Electronics, IEEE Trans on, 2011, 58(7), pp. 2872–2882.

[3] T.Paul. Chow, “SiCand GaN High- Voltage Power Switching Devices”, Materials Science Forum, vol. 338 -342, Pp 1155-11 60, 2000.

[4] Yuan-Bo Guo, K. P. Bhat, A. Aravamudhan, D. C. Hopkins, D. R. Hazelmyer, “High current and thermal transient design of a SiC SSPC for aircraft application,” Applied Power Electronics Conference and Exposition (APEC), 2011 26th Annual IEEE, 2011, pp. 1290–1297.

[5] T. Nakamura, M. Sasagawa, Y. Nakano, T. Otsuka, M. Miura, “Large current SiC power devices for automobile applications,” Power Electronics Conference (IPEC), 2010 International, 2010, pp. 1023–1026.

[6] Hui Zhang, L. M. Tolbert, B. Ozpineci, “Impact of SiC Devices on Hybrid Electric and Plug-In Hybrid Electric Vehicles,” Industry Applications, IEEE Trans on, 2011, pp. 912–921.

[7] C. N. M. Ho, H. Breuninger, S. Pettersson, G. Escobar, F. Canales,“A comparative performance study of an interleaved boost converter using commercialized Si and SiC diodes for PV applications,” Power Electronics and ECCE Asia (ICPE & ECCE), 2011 IEEE 8th International Conference on, 2011, pp. 1190–1197.

[8] D. C. Sheridan, A. Ritenour, R. Kelley, V. Bondarenko, J. B. Casady, “Advances in SiC VJFETs for renewable and high-efficiency power electronics applications,” Power Electronics Conference (IPEC), 2010 International, 2010, pp. 3254–3258.

[9] Hui Zhang, L. M. Tolbert, Jung Hee Han, M. S. Chinthavali, F. Barlow, “18 kW three phase inverter system using hermetically sealed SiC phase-leg power modules,” Applied Power Electronics Conference and Exposition (APEC), 2010 25th Annual IEEE, 2010, pp. 1108–1112.

[10] T. J. Han, J. Nagashima, Sung Joon Kim, et al, “High density 50 kW SiC inverter systems using a JFET based six-pack power module,” Power Electronics and ECCE Asia (ICPE & ECCE), 2011 IEEE 8th International Conference on, 2011, pp. 764–769.

[11] D. Peftitsis, G. Tolstoy, A. Antonopoulos, et al, “High-power modular multilevel converters with SiC JFETs,” Energy Conversion Congress and Exposition (ECCE), 2010 IEEE, 2010, pp. 2148–2155.

[12] D. Bortis, B. Wrzecionko, J. W. Kolar, “A 120°C ambient temperature forced air-cooled normally-off SiC JFET automotive inverter system,” Applied Power Electronics Conference and Exposition (APEC), 2011 26th Annual IEEE, 2011, pp. 1282–1289.

[13] C. Wilhelm, D. Kranzer, B. Burger, “Development of a highly compact and efficient solar inverter with Silicon Carbide transistors,” Integrated Power Electronics Systems (CIPS), 2010 6th International Conference on, 2010, pp. 1–6.

[14] R. Robutel, C. Martin, et al, “Integrated common mode capacitors for SiC JFET inverters,” Applied Power Electronics Conference and Exposition (APEC), 2011 26th Annual IEEE, 2011, pp. 196–202.

[15] J. Millán, P. Godignon, X. Perpiñà, A. Pérez-Tomás and J. Rebollo, "A Survey of Wide Bandgap Power Semiconductor Devices," IEEE Transactions on Power Electronics, vol. 29, no. 5, pp. 2155-2163, May 2014.

[16] E. Bahat-Treidel, “GaN Based HEMTs for High Voltage Operation,” Technischen Universität Berlin, Germany, 2012.

[17] J. D. Van Wyk and F. C.Lee, “On a future for power electronics,” IEEE J. Emerg. Sel. Topics Power Electron., vol. 1, no. 2, pp. 59–72, June, 2013.

[18] B. J. Baliga, Fundamentals of power semiconductor devices. Springer, 2010.

[19] A. K. Agarwal, S. S. Mani, S. Seshadri, J. B. Cassady, P. A. Sanger, C. D. Brandt, and N. Saks, “SiC power devices,” Naval Research Reviews, 51(1), pp. 14–21, 1999.

[20] “Figures of Merit,” EEEnet: Electronics for Extreme Environments, http://www.eeenet.org/figs_of_merit.asp.

[21] B. Ozpineci, L. M. Tolbert, S. K. Isalm, and M. Chinthavali, "Comparison of Wide Bandgap Semiconductors for Power Electronics Applications;" *Proccedings of the 10th European Conference on Power Electronics and Applications*, pp. 257-264. September 2003.

[22] K. Shenai, R. S. Scott, and B. J. Baliga, “Optimum semiconductors for high power electronics,” IEEE Transactions on Electron Devices, 36(9), pp. 1811-1823, 1989.

[23] J. Biela, M. Schweizer, S. Waffler, J. W. Kolar, “SiC versus Si—Evaluation of Potentials for Performance Improvement of Inverter and DC–DC Converter Systems by SiC Power Semiconductors,” Industrial Electronics, IEEE Trans on, 2011, 58(7), pp. 2872–2882.

[24] D. Peftitsis, R. Baburske, J. Rabkowski, et al., “Challenges regarding parallel-connection of SiC JFETs,” Power Electronics and ECCE Asia (ICPE & ECCE), 2011 IEEE 8th International Conference on, 2011, pp. 1095–1101.

[25] S. Waffler, S. D. Round, J. W. Kolar, “High temperature (>200°C) isolated gate drive topologies for Silicon Carbide (SiC) JFET,” Industrial Electronics (IECON), 2008 34th Annual Conference of IEEE, pp.2867-2872, 10-13 Nov. 2008.

[26] Ruxi Wang, Puqi Ning, D. Boroyevich, et al., “Design of hightemperature SiC three-phase AC-DC converter for >100°C ambient temperature,” Energy Conversion Congress and Exposition (ECCE), 2010 IEEE, 2010, pp. 1283–1289.

[27] J. Hornberger, A. B. Lostetter, K. J. Olejniczak, T. McNutt, et al., “Silicon-carbide (SiC) semiconductor power electronics for extreme high-temperature environments,” Aerospace Conference, 2004. Proceedings. 2004 IEEE, vol.4, no., pp. 2538-2555, 13-13 March 2004.

[28] F. Dahlquist, “Junction barrier Schottky rectifiers in silicon carbide,”Ph.D. dissertation, Royal Institute of Technology, Brinellvägen, Sweden, 200

[29] C. Bodeker, T. Vogt, and N. Kaminski, “Stability of SiC Schottky diode against leakage current thermal runaway,” Proc. Int. Symp. Power Semicond. Devices ICs, 2015, pp. 245–248.

[30] A. Agarwal, "Advances in SiC MOSFET performance*", ECPE SiC & GaN Forum Potential of Wide Bandgap Semicond. Power Electron*. Appl., 2011.

[31] F. Wang, G. Wang, A.Q. Huang, W. Yu, and X. Ni, “Design and operation of a 3.6 kV high performance solid state transformer based on 13 kV SiC MOSFET and JBS diode,” Proc. IEEE ECCE, 2014, pp. 4553–4560.

[32] T. Kimoto, “Ultrahigh-voltage SiC devices for future power infrastructure,” Proc. ESSDERC, Sept. 2013, pp. 22–29.

[33] Wondrak, W., Niemann, E., Held, R., Constapel, R., & Kroetz, G. (1998). SiC devices for power and high-temperature applications, Vol. 1, pp. 153 – 156).

[34] X. Wang and J. A. Cooper. Jr., “Optimization of JTE edge terminations for 10 kV power devices in 4H SiC,” in Mat. Sci. Forum, vol. 457–460, pp. 1257–1260, 2003.

[35] W. Sung, J. Baliga, and A. Q. Huang, “Area-efficient bevel-edge termination techniques for SiC high-voltage devices,” IEEE Trans. Electron. Devices, vol. 63, no. 4, pp.1630–1636, April, 2016.

[36] Ralf Siemieniec and Uwe Kirchner, “The 1200V Direct-Driven SiC JFET power switch,” EPE 2011.

[37] Wang, J., Zhao, T., Li, J., Huang, A. Q., Callanan, R., Husna, F., & Agarwal, A. K. (2008, August). Characterization, Modeling, and Application of 10-kV SiC MOSFET. Electron Devices, IEEE Transactions on, 55(8), 1798 – 1806.

[38] S. Guo, L. Zhang, Y. Lei, X. Li, F. Xue, W. Yu, and A. Q. Huang, “3.38 MHz operation of 1.2 kV SiC MOSFET with integrated ultra-fast gate drive,“ IEEE 3rd Workshop on Wide Bandgap Power Devices and Applications (WiPDA), 2015, pp. 390–395.

[39] X. Li, K. Tone, L. H. Cao, P. Alexandrov, L. Fursin, and J. H. Zhao, “Theoretical and experimental study of 4H-SiC junction edge termination,” Mater. Sci. For., vol. 338-342, pp. 1375-1379, 2000.

[40] K. Vechalapu, S. Bhattacharya, E. Van Brunt, S. H. Ryu, D. Grider and J. W. Palmour, "Comparative Evaluation of 15-kV SiC MOSFET and 15-kV SiC IGBT for Medium-Voltage Converter Under the Same dv/dt Conditions," in *IEEE Journal of Emerging and Selected Topics in Power Electronics*, vol. 5, no. 1, pp. 469-489, March 2017.

[41] M. K. Das, R. Callanan, D. C. Capell, B. Hull, F. Husna, J. Richmond, M. O’loughlin, M. J. Paisley, A. Powell, and Q. Zhang, “State of the art 10 kV NMOS transistors,” Proc. Int. Symp. Power Semicond. Devices ICs, 2008, pp. 253–255.

[42] M. K. Das, J. Zhang, R. Callanan, C. Capell, J. Clayton, M. Donofrio.S, K. Haney, F. Husna, C. Jonas, J. Richmond, and J. J. Sumakeris, “A 13 kV 4H-SiC n-channel IGBT with low Rdiff, on and fast switching,” Mat. Sci. Forum, vol. 600–603, pp. 1183–1186, 2009.

[43] X. Wang and J. A. Cooper, “High-voltage N-Channel IGBTs on freestanding 4H-SiC epilayers,” IEEE Trans. Electron. Devices, vol. 57, no. 2, Feb., 2010.

[44] S. Ryu, C. Capell, L. Cheng, C. Jonas, A. Gupta, M. Donofrio, J. Clayton, M. O'Loughlin, A. Burk, D. Grider, A. Agarwal, J. Palmour, and A. Hefner, “Ultra high voltage (>12 kV), high performance 4H-SiC IGBTs,” Proc. Int. Symp. Power Semicond. Devices ICs, 2012, pp. 257– 260.

[45] S.Ryu, C.Capell, C.Jonas, Y.Lemma, M.O'Loughlin, J.Clayton, E.Van Brunt, K.Lam, J.Richmond, A. Burk, D.Grider, S.Allen, J.Palmour, A.Agarwal, A.Kadavelugu, and S.Bhattacharya, “Ultra high voltage IGBTs in 4H-SiC,” Proc. IEEE WiPDA, 2013, pp. 36–39.

[46] E. V. Brunt, L. Cheng, M. O’Loughlin, C. Capell, C. Jonas, K. Lam, J. Richmond, V. Pala, S. Ryu, S. T. Allen, A. A. Burk, J. W. Palmour, and C. Scozzie, “22 kV, 1cm^2, 4H-SiC n-IGBTs with improved conductivity modulation,” Proc. Int. Symp. Power Semicond. Devices ICs, 2014, pp. 358–361.

[47] E.Van Brunt, L.Cheng, M.J. O'Loughlin, J.Richmond, V.Pala, J.Palmour, C.W.Tipton, and C.Scozzie , “27 kV, 20 A 4H-SiC nIGBTs,” Mat. Sci. Forum, vol. 821–823, pp. 847–850, 2015.

[48] K. Fukuda et al., “Development of ultra high voltage SiC power devices,” IEEE Trans. Electron. Devices, vol. 62, no. 2, pp. 396–404, Feb., 2015.

[49] Q. Zhang, H.-R. Chang, M. Gomez, C. Bui, E. Hanna, J. A. Higgins, T. Isaacs-Smith, and J. R. Williams, “10 kV trench gate IGBTs on 4HSiC,” Proc. Int. Symp. Power Semicond. Devices ICs, 2005, pp. 303– 306.

[50] Q. Zhang, C. Jonas, S. Ryu, A. Agarwal, and J. Palmour, “New improvement results on 7.5 kV 4H-SiC p-IGBTs with Rdiff, of 26 mΩ.cm^2 at 25°C,” Proc. Int. Symp. Power Semicond. Devices ICs, 2007, pp. 281–284.

[51] L. Cheng, A. Agarwal, M. O’Loughlin, C. Capell, A.Burk, J. Palmour, A. Ogunniyi, H. O’Brien, and C. Scozzie, “Advanced silicon carbide gate turn-off thyristor for energy conversion and power grid applications,” Proc. IEEE ECCE, 2012, pp. 2249–225.

[52] Zhang, Q., Agarwal, A. K., Capell, C., O’Loughlin, M., Burk, A. A., Palmour, J. W., … Scozzie, C. J., “SiC super GTO thyristor technology development - Present status and future perspective, ” Chicago, IL., 2011, pp. 1530 – 1535.

[53] A. Q. Huang, C. Peng, and X. Song, “Design and development of a 7.2 kV/200 A hybrid circuit breaker based on 15 kV SiC emitter turn-off (ETO) thyristor,” Proc. IEEE ESTS, 2015, pp. 306–311.

[54] Cheng, L., Agarwal, A. K., O’Loughlin, M., Capell, C., Burk, A. A., Palmour, J. W., … Scozzie, C. J., “Advanced silicon carbide gate turn-off thyristor for energy conversion and power grid applications, ” Raleigh, NC., 2012, pp. 2249 – 225.